ACCOUNTS
of chemical research

Molecular Water Oxidation Mechanisms Followed by Transition Metals: State of the Art

XAVIER SALA,[†] SOMNATH MAJI,[‡] ROGER BOFILL,[†] JORDI GARCÍA-ANTÓN,[†] LLUÍS ESCRICHE,[†] AND ANTONI LLOBET*,[†,‡]

[†]*Departament de Química, Universitat Autònoma de Barcelona, Cerdanyola del Vallès, 08193 Barcelona, Spain, and* [‡]*Institute of Chemical Research of Catalonia (ICIQ), Av. Països Catalans, 16, 43007 Tarragona, Spain*

RECEIVED ON JULY 26, 2013

CONSPECTUS

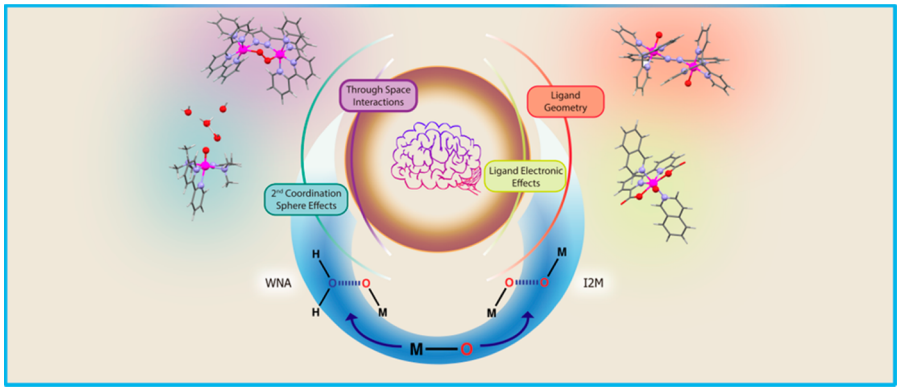

One clean alternative to fossil fuels would be to split water using sunlight. However, to achieve this goal, researchers still need to fully understand and control several key chemical reactions. One of them is the catalytic oxidation of water to molecular oxygen, which also occurs at the oxygen evolving center of photosystem II in green plants and algae. Despite its importance for biology and renewable energy, the mechanism of this reaction is not fully understood.

Transition metal water oxidation catalysts in homogeneous media offer a superb platform for researchers to investigate and extract the crucial information to describe the different steps involved in this complex reaction accurately. The mechanistic information extracted at a molecular level allows researchers to understand both the factors that govern this reaction and the ones that derail the system to cause decomposition. As a result, rugged and efficient water oxidation catalysts with potential technological applications can be developed.

In this Account, we discuss the current mechanistic understanding of the water oxidation reaction catalyzed by transition metals in the homogeneous phase, based on work developed in our laboratories and complemented by research from other groups. Rather than reviewing all of the catalysts described to date, we focus systematically on the several key elements and their rationale from molecules studied in homogeneous media. We organize these catalysts based on how the crucial oxygen–oxygen bond step takes place, whether via a water nucleophilic attack or via the interaction of two M–O units, rather than based on the nuclearity of the water oxidation catalysts. Furthermore we have used DFT methodology to characterize key intermediates and transition states. The combination of both theory and experiments has allowed us to get a complete view of the water oxidation cycle for the different catalysts studied. Finally, we also describe the various deactivation pathways for these catalysts.

1. Introduction

During the last 5 years, there has been an explosion of reports in the field of water oxidation catalyzed by transition metals fueled in part by the promise of a potentially viable clean and cheap energy source, alternative to today's fossil fuels. The field has benefited from a significant increase in funding from central governments, at least in the US, which has realized not only the urgency but also its potential payback. In addition, the possibility of a C-neutral fuel could also solve the global warming issue. On the other

Published on the Web 12/11/2013 www.pubs.acs.org/accounts
10.1021/ar400169p

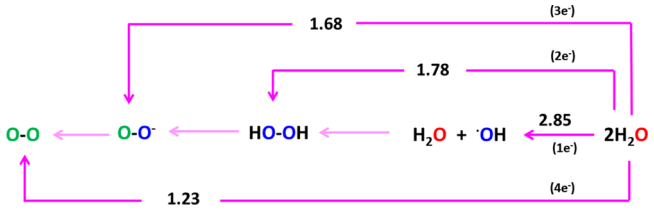

FIGURE 1. Oxygen Latimer diagram at pH = 0.0 with $E°$ values vs NHE. Oxygen atoms in *formal* oxidation state −2 are labeled in red, −1 in blue, and 0 in green. In parentheses is indicated the number of electrons withdrawn from two water molecules.

hand from a philosophical perspective, it does not seem right that even today the main use of oil is just burning it. Oil should be regarded as a very valuable commodity for the construction of the new materials of the future.

A potentially clean alternative to fossil fuels is water splitting by sunlight.

$$2H_2O \xrightarrow{h\nu} 2H_2 + O_2 \qquad (1)$$

From an electrochemical perspective, this reaction can be divided in two half reactions, water oxidation and proton reduction, as indicated in the equations below at pH = 0 (all redox potentials presented in the present paper have been converted vs. NHE):

$$2H_2O \rightarrow O_2 + 4H^+ + 4e^- \qquad E° = 1.23V \qquad (2)$$

$$2H^+ + 2e^- \rightarrow H_2 \qquad E° = 0.0V \qquad (3)$$

The oxidation of water to dioxygen is thus one of the key reactions that need to be fully understood in order to be able to couple it to proton reduction catalysis and light harvesting and end up with a water splitting device.

During the last 5 years, there have been important developments with respect to the design of new transition metal complexes, characterized by different ligand sets and architectures that have been shown to be capable of making dioxygen from water in the presence of an excess of a sacrificial oxidant. This set of water oxidation catalysts (WOCs) provides a relatively large body of information that allows visualization of the variety of strategies that can be used to achieve this goal, as well as the numerous problems associated with this catalytic process including deactivation pathways.

2. The Basics

A Latimer diagram for oxygen is presented in Figure 1. From the diagram, it can be deduced that water can be oxidized in four different manners depending on the number of electrons removed. The four electron process is the lower energy

SCHEME 1. O−O Bond Formation Pathways Promoted by Transition Metal Complexes in High Oxidation States: (left) Water Nucleophilic Attack (WNA) and (right) Interaction of Two M−O Units (I2M)

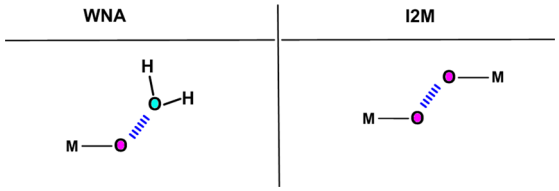

path and is the one occurring also at the oxygen evolving center of photosystem II (OEC-PSII) in green plants and algae.[1] This low energy thermodynamics contrasts with the increase of molecular complexity. For the case of the $4e^-$ removal, four O−H bonds from two water molecules have to be broken and an O−O bond has to be formed. Thus catalysts that need to perform this reaction will have to unavoidably deal with the removal of multiple electrons and protons. In this respect, there are a number of transition metal complexes containing aqua ligands with general formula $[M^{n+}-OH_2]$ that can suffer the reversible removal of $1H^+$ and $1e^-$ and generate the corresponding $[M^{(n+1)+}-OH]$ complexes and thus represent an example of the former. The $[Ru-OH_2]$ polypyridyl complexes constitute a paradigmatic family of this type of complexes that has been thoroughly studied over the last three decades.[2] The Ru−aqua polypyridyl complexes can lose protons and electrons and easily reach higher oxidation states within a narrow potential range, thanks to the σ- and π-donation character of the oxo group that stabilizes those higher oxidation states. Additionally the removal of one proton and one electron (H-atom) precludes Coulombic charge build up that would otherwise take place in simple outer sphere electron transfer processes and that would strongly destabilize the complex. Thus proton coupled electron transfer (PCET) offers low energy pathways for the oxidative process and thus ensures relatively rapid reaction kinetics for the whole water oxidation reaction. The use of PCET to access low energy pathways is also played by Nature in the OEC-PSII[1] within the so-called redox-leveling. In addition to the removal of protons and electrons, the oxidation of water to dioxygen requires the formation of an O−O bond. Besides the OEC-PSII, it has been shown recently that chlorite dismutases also carry out this reaction.[3] Formally, from a mechanistic perspective, the formation of an oxygen−oxygen bond promoted by transition metal complexes can be classified taking into account whether a free water molecule participates in the formation of the aforementioned bond. From this perspective, two possibilities

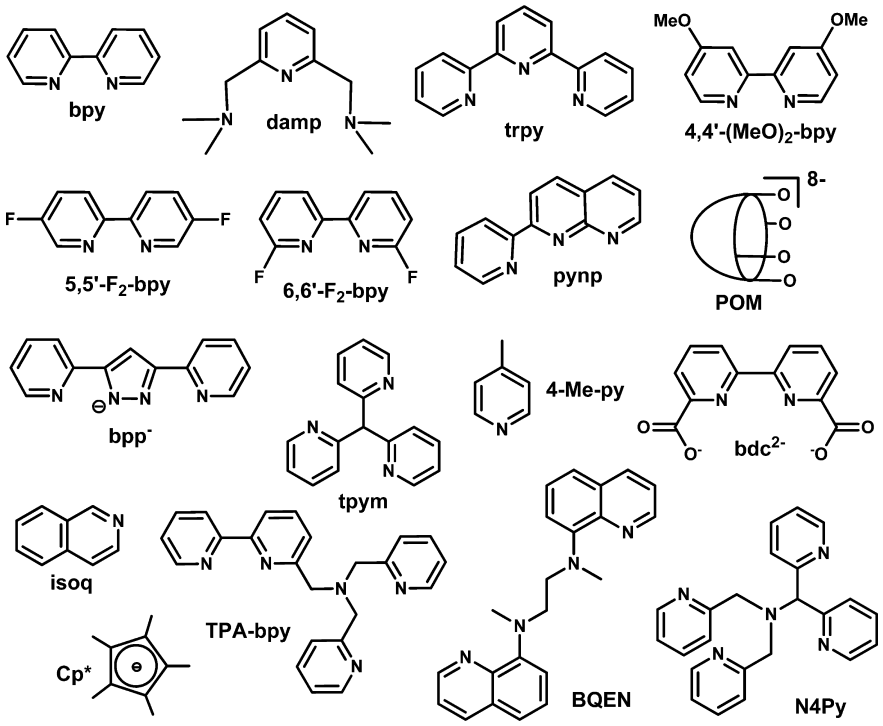

FIGURE 2. Ligands discussed in this Account.

exist: water nucleophilic attack (WNA) and interaction of two M−O units (I2M) as depicted in Scheme 1.

3. Water Nucleophilic Attack, WNA

3.1. Mononuclear Monoaqua Complexes. A significant number of Ru water oxidation catalysts have been reported and are proposed to undergo a reaction mechanism involving WNA.[4] One of them is the $[Ru^{II}(damp)(bpy)(H_2O)]^{2+}$, $\mathbf{1}^{2+}$ (damp = 2,6-bis(dimethylamino)pyridine; bpy = 2,2′-bipyridine; all ligands discussed in this Account are drawn in Figure 2) whose mechanistic details have been reported very recently.[5] The damp ligand, containing two strongly σ-donating tertiary amine coordinating groups, provides the right electronic environment to stabilize higher oxidation states together with extensive H-bonding (see Figure 3 for a calculated DFT structure). Thus the complex undergoes two sequential H^+/e^- losses at relatively close potentials at pH = 1.0,

$$[Ru^{II}(damp)(bpy)(H_2O)]^{2+} - 1H^+ - 1e^- \rightarrow [Ru^{III}(damp)(bpy)(OH)]^{2+} \qquad E^\circ = 0.83V \quad (4)$$

$$[Ru^{III}(damp)(bpy)(OH)]^{2+} - 1H^+ - 1e^- \rightarrow [Ru^{IV}(damp)(bpy)(O)]^{2+} \qquad E^\circ = 0.97V \quad (5)$$

In addition as shown spectroscopically and electrochemically, the complex can lose one more electron and reach Ru(V),

$$[Ru^{IV}(damp)(bpy)(O)]^{2+} - 1e^- \rightarrow [Ru^{V}(damp)(bpy)(O)]^{3+} \qquad E^\circ = 1.79V \quad (6)$$

At this point, Ru(V) reacts with a solvent water molecule to generate the corresponding hydroperoxide as indicated in the following equation:

$$[Ru^{V}(damp)(bpy)(O)]^{3+} + H_2O \rightarrow [Ru^{III}(damp)(bpy)(OOH)]^{2+} + H^+ \qquad \Delta G^\circ = 20.7kcal/mol \quad (7)$$

The formation of the hydroperoxide intermediate from Ru(V) is accompanied formally with a two electron reduction of the metal center and thus generates [Ru(III)−OOH], which is a relatively inert (low spin d^5 ion) and stable complex. At this point, an oxidative activation is needed for the catalytic cycle to proceed as indicated in the following equation:

$$[Ru^{III}(damp)(bpy)(OOH)]^{2+} - 1H^+ - 1e^- \rightarrow [Ru^{IV}(damp)(bpy)(OO)]^{2+} \quad (8)$$

For this particular system, this step represents the rate-determining step (rds). Now Ru(IV) has sufficient oxidative capacity to accept two electrons from the peroxido bonded ligand generating Ru(II), ejecting molecular

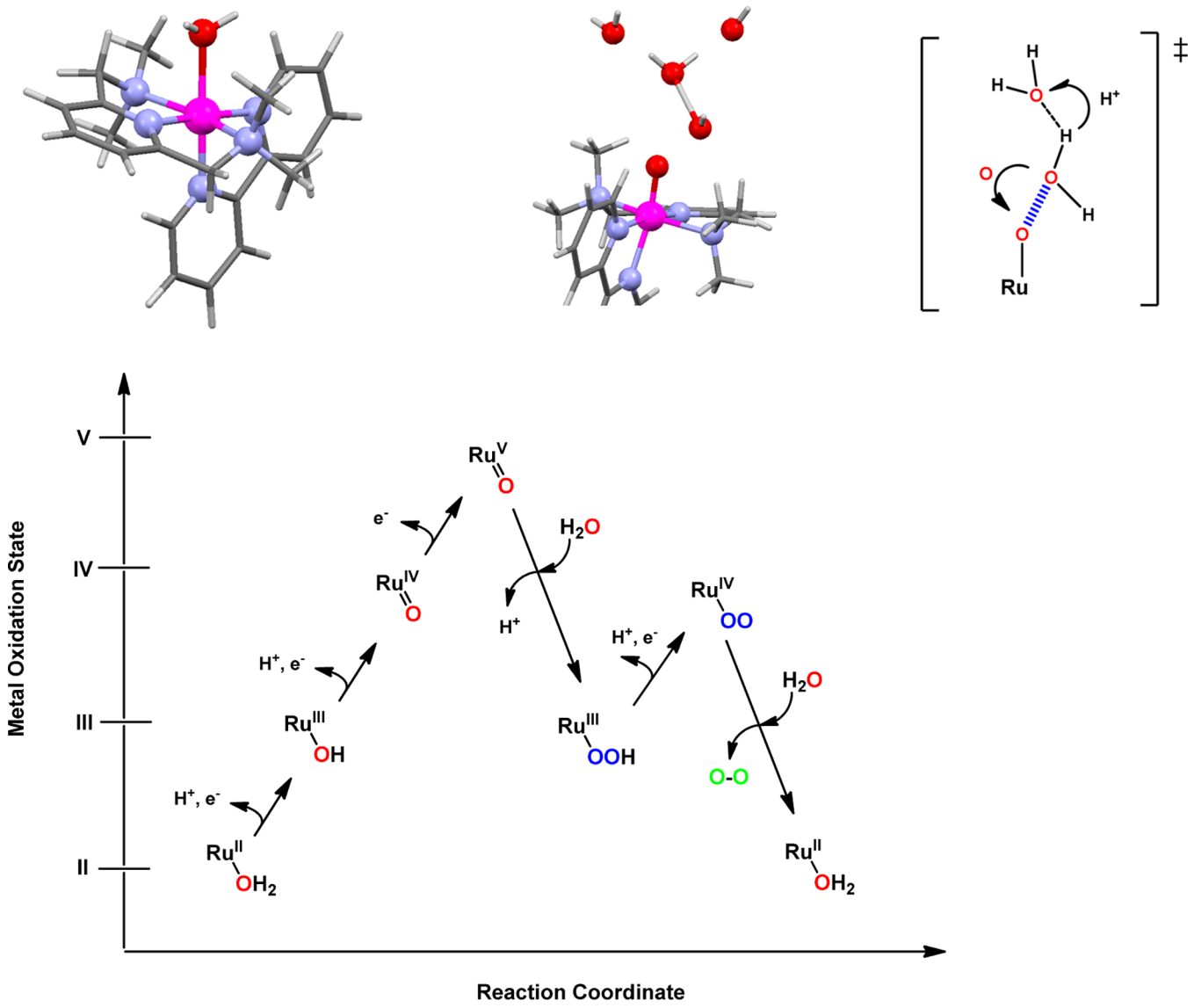

FIGURE 3. (top, left) Capped stick representation of $[Ru^{II}(damp)(bpy)(H_2O)]^{2+}$, $\mathbf{1}^{2+}$, DFT calculated structure. Balls are used for Ru, for the atoms of its first coordination sphere, and for additional selected atoms of interest. Color codes: Ru = fuchsia; N = blue; O = red; C = gray; H = white. (top, center) Detail of the transition state structure for the O−O formation step that includes three additional water molecules. (top, right) Drawing showing the atom proton transfer (APT) mechanism in the TS. (bottom) "Roller coaster" water oxidation mechanism catalyzed by $\mathbf{1}^{2+}$.

oxygen, and closing the catalytic cycle.

$$[Ru^{IV}(damp)(bpy)(OO)]^{2+} + H_2O \rightarrow [Ru^{II}(damp)(bpy)(H_2O)]^{2+} + O{=}O \quad (9)$$

The whole mechanistic proposal is presented in Figure 3, where a plot of the formal oxidation states of the metal center as a function of reaction coordinate is depicted. We termed this type of mechanism as a "roller coaster" mechanism given the increasing and decreasing values of the metal oxidation state within the catalytic cycle. This type of diagram is useful because it allows identification of the main phases of the process, which are oxidative activation of the initial complex, O−O bond formation, and dioxygen ejection concomitant with regeneration of the initial species. This in turn allows visualization of ligand effects at the different stages as will be shown in subsequent sections. This catalytic scheme is nowadays proposed for a variety of mononuclear monoaqua transition metal WOCs.[6]

We are using the DFT description in this Account when the data reported is in agreement with experiment, thus providing a complementary view that is extremely valuable to visualize the whole mechanism.

3.2. Overoxidation and Base Effects. A very interesting question within the WNA mechanism refers to the activity of

the high oxidation states and their accessibility. For the particular case of the Ru−damp complex, a further oxidation from Ru(V) to Ru(VI) is not observed experimentally, but it is computationally calculated to appear at 2.54 V.

$$[Ru^{VI}(damp)(bpy)(O)]^{4+} + 1e^- \rightarrow [Ru^{V}(damp)(bpy)(O)]^{3+} \qquad E^{\circ}_{calc} = 2.54V \tag{10}$$

The Ru(VI) could now undergo a WNA to generate the corresponding Ru(IV)−OOH complex,

$$[Ru^{VI}(damp)(bpy)(O)]^{4+} + H_2O \rightarrow [Ru^{IV}(damp)(bpy)(OOH)]^{3+} + H^+ \tag{11}$$

The activation energy calculated for this step is 5 kcal/mol lower than that for the related reaction at oxidation state V (eq 7). This result is intuitively reasonable assuming that the higher the oxidation state the more electrophilic character of the oxygen atom of the Ru−O bond. Thus a key property that will strongly influence the reactivity of the complexes is the electronic structure of the Ru−O moiety. This electronic structure will be mainly influenced by the oxidation state and by the auxiliary ligands that complete the coordination sphere of the metal center (*vide infra*).

Another key factor that strongly influences reactivity is the second coordination sphere interactions such as hydrogen bonding or base effects. An example of the former is remarkably illustrated also in the Ru-damp case, particularly in the transition state (TS) of the O−O bond formation step that is also the rds. For this step, there is a need for three additional water molecules to lower the TS energy, that is,

$$[Ru^{V}(damp)(bpy)(O)]^{3+} + 4H_2O \rightarrow \{[Ru(damp)(bpy)(O\cdots OH_2)(H_2O)_3]^{3+}\}^{TS} \rightarrow [Ru^{III}(damp)(bpy)(OOH)]^{2+} + H_3O^+ + 2H_2O \tag{12}$$

The role of the additional water molecules is to generate a network of H-bonds and also acting as a base to promote proton shuttling (see Figure 3), which is a potential mimic for fast proton transfer in OEC-PSII.[1] A quantitative example of this base effect over kinetics of water oxidation has been described for a related mononuclear complex $[Ru(Mebimpy)(bpy)(H_2O)]^{2+}$, $\mathbf{2}^{2+}$, (Mebimpy=2,6-bis(1-methylbenzimidazol-2-yl)pyridine),[7] where depending on the base added the velocity increases by nearly 2 orders of magnitude.

3.3. Electronic Effects and Through Space Interactions. The $[Ru(trpy)(bpy)(H_2O)]^{2+}$ complex, $\mathbf{3}^{2+}$ (trpy = 2,2′:6′,2″-terpyridine), follows a WNA mechanism where the rds has been shown to be the last step, the ejection of molecular oxygen accompanied formally with the reduction of $[Ru^{IV}-OOH]$ to $[Ru^{II}]$ ($Ru^{IV}-OO + H_2O \rightarrow Ru^{II}-OH_2 + O_2$). Replacement of the bpy ligand by the strongly electron donating 4,4′-$(MeO)_2$-bpy, $[Ru(trpy)(4,4'-(MeO)_2\text{-bpy})(H_2O)]^{2+}$, $\mathbf{4}^{2+}$, is proposed to switch the rds of the catalytic cycle to the one-electron oxidation step from $[Ru^{IV}-OO]$ to $[Ru^{V}-OO]$.[8] This is because the MeO group produces a dual effect: it decreases the reduction capacity of the $[Ru^{IV}-OO]$ intermediate and at the same time it facilitates access to a higher oxidation state $[Ru^{V}-OO]$.

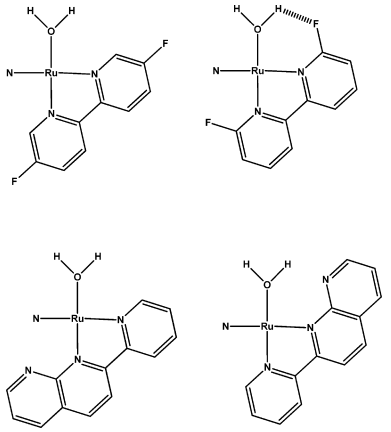

FIGURE 4. (top) Drawing of the equatorial plane constituted by the bidentate ligand and the Ru−aqua group for complexes $[Ru^{II}(trpy)(5,5'-F_2\text{-bpy})(H_2O)]^{2+}$, $\mathbf{5}^{2+}$, and $[Ru^{II}(trpy)(6,6'-F_2\text{-bpy})(H_2O)]^{2+}$, $\mathbf{6}^{2+}$. (bottom) *cis*- and *trans*-$[Ru^{II}(trpy)(pynp)(H_2O)]^{2+}$, *cis*- and *trans*-$\mathbf{7}^{2+}$. Only the N atom of the trpy ligand that is situated in the mentioned equatorial plane is shown.

An example of both electronic and through space interactions is nicely shown for the case of $[Ru(trpy)(5,5'-F_2\text{-bpy})(H_2O)]^{2+}$, $\mathbf{5}^{2+}$, and $[Ru(trpy)(6,6'-F_2\text{-bpy})(H_2O)]^{2+}$, $\mathbf{6}^{2+}$.[9] Whereas $\mathbf{5}^{2+}$ can only influence the reactivity via the electronic perturbation of the bpy ring, $\mathbf{6}^{2+}$ can additionally interact through space with the $[Ru-OOH]$ and $[Ru-OH_2]$ group, as depicted in Figure 4, and strongly affects the kinetics of the process. Another example of a dramatic effect due to through space interaction is the case of *cis*- and *trans*-$[Ru^{II}(trpy)(pynp)(H_2O)]^{2+}$, *cis*- and *trans*-$\mathbf{7}^{2+}$ (pynp = 2-(2-pyridyl)-1,8-naphthyridine). While the *cis*-$\mathbf{7}^{2+}$ works relatively efficiently, similar to $\mathbf{3}^{2+}$, the *trans*-$\mathbf{7}^{2+}$ isomer is practically inactive. The different behavior is ascribed to the destabilization of higher oxidation states produced by the electronic pair of the noncoordinating N-atom of the naphthyridine group (see Figure 4).[10,11]

3.4. Multiple Ru−Aqua Bonds. An interesting family of water oxidation catalysts is the one that contains multiple

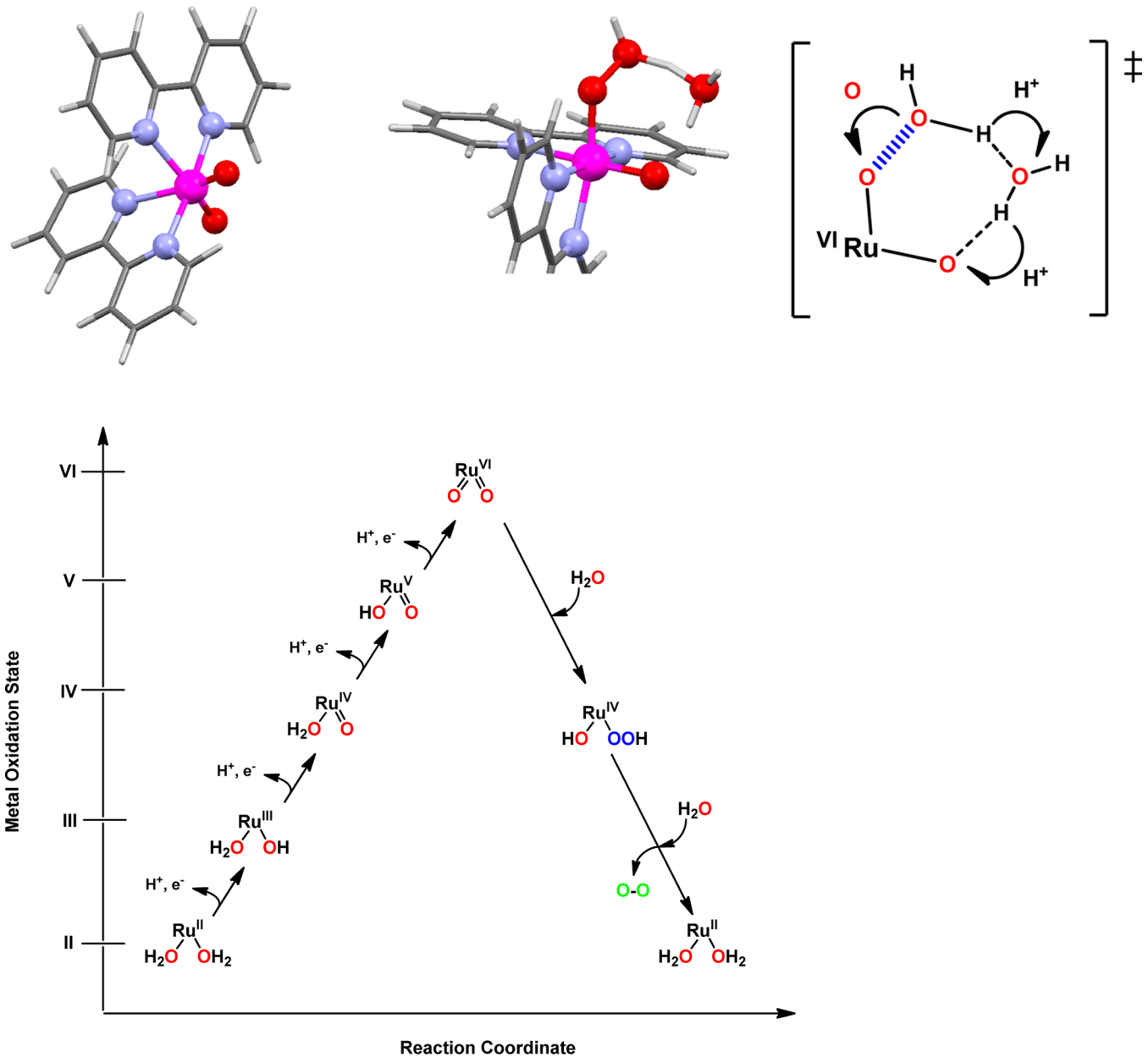

FIGURE 5. (top, left) Capped stick representation of [*cis*-$[Ru^{VI}(bpy)_2(O)_2]^{2+}$ DFT calculated structure. (top, center) Detail of the transition state structure for the O−O formation step that includes one additional water molecule. (top, right) Drawing showing the A2PT mechanism in the TS. (bottom) "Volcano" water oxidation mechanism catalyzed by $\mathbf{8}^{2+}$.

Ru−aqua bonds. This can be achieved with mononuclear complexes as is the case of *cis*-$[Ru^{II}(bpy)_2(H_2O)_2]^{2+}$, $\mathbf{8}^{2+}$,[12] or with polynuclear complexes where the metal centers are connected through a bridging ligand (BL) as is the case of the blue dimer *cis,cis*-$\{[Ru^{III}(bpy)_2(H_2O)]_2(\mu\text{-}O)\}^{4+}$, $\mathbf{9a}^{4+}$,[13] and the $[Ru_4O_4(OH)_2(H_2O)_4(\gamma\text{-}SiW_{10}O_{36})_2]^{10-}$, $\mathbf{9b}^{10-}$ ($(\gamma\text{-}SiW_{10}O_{36})^{8-}$ = POM).[14] In both cases, the BLs used are the oxido group, which allows production of significant electronic coupling through the Ru metals, and as a consequence, the metals will behave in a cooperative manner. The absence of electronic coupling between the metal centers would produce complexes whose behavior would closely resemble that of the mononuclear counterparts.

For the bis-aqua complex $\mathbf{8}^{2+}$, there is spectroscopic and electrochemical evidence that the complex undergoes four successive one-electron oxidations that overall are coupled to the removal of $4H^+$,

$$cis\text{-}[Ru^{II}(bpy)_2(H_2O)_2]^{2+} - 4H^+ - 4e^- \rightarrow cis\text{-}[Ru^{VI}(bpy)_2(O)_2]^{2+} \quad (13)$$

For this complex, ^{18}O labeling experiments unambiguously show that upon reaching Ru(VI) the complex undergoes a

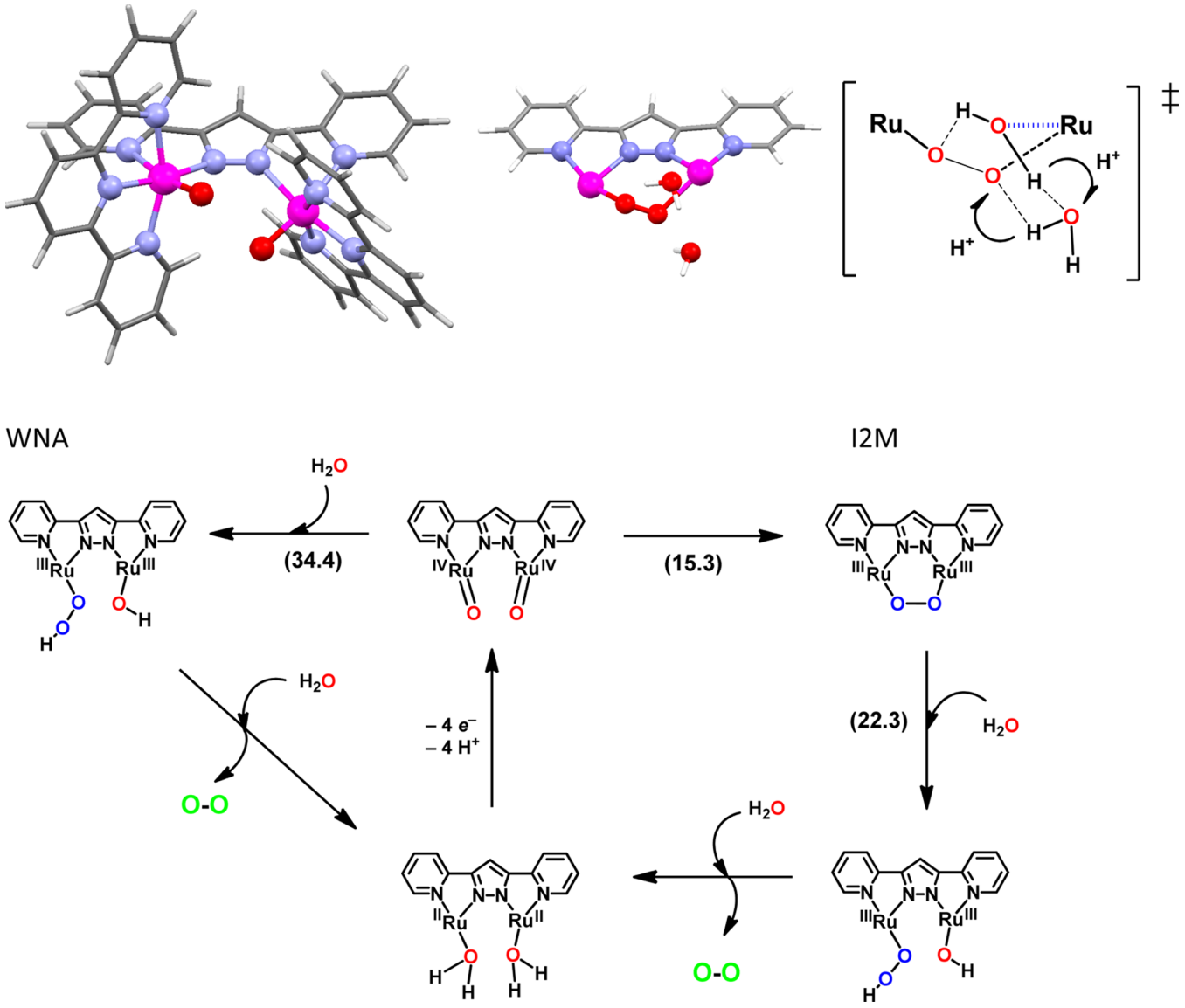

FIGURE 6. (top, left) Capped stick representation of *in,in*-{[Ru^{IV}(trpy)(O)]$_2$(μ-bpp)}$^{3+}$ DFT calculated structure. (top, center) Detail of the transition state structure for the terminal Ru–hydroperoxide formation step (I2M) that includes one additional water molecule. (top, right) Drawing of TS. (bottom) Water oxidation mechanism catalyzed by **10**$^{3+}$, showing the WNA and I2M mechanisms.

WNA forming the corresponding hydroperoxido complex as indicated in the following equation,

$$cis\text{-}[Ru^{VI}(bpy)_2(O)_2]^{2+} + H_2O \rightarrow cis\text{-}[Ru^{IV}(bpy)_2(OOH)(OH)]^{2+} \quad (14)$$

The catalytic cycle proposed is presented in a graphical manner in Figure 5 and constitutes one example of the so-called "volcano mechanism". One interesting feature of this system is the presence of two Ru–aqua groups that give a high degree of covalency to the O–Ru–O moiety. The presence of two water molecules bonded to the same metal center allows it to obtain a Ru(V) oxidation state that is relatively stable and further allows it to reach even higher oxidation states to Ru(VI). Another interesting feature of this system is once again the role of an additional H_2O to stabilize the transition state involving an A2PT (atom two proton transfer) type of mechanism for the reaction shown in eq 14.

Whereas for **8**$^{2+}$, the metal center needs to cycle among five different oxidation states, the presence of multiple Ru–aqua groups bonded through oxido bridges as in Ru–POM **9b**$^{10-}$, allow one to obtain a system where the metal center needs to cycle only through two different oxidation states and thus the demands with regard to the stability of multiple oxidation states here is much less stringent. In this case, DFT together with experimental

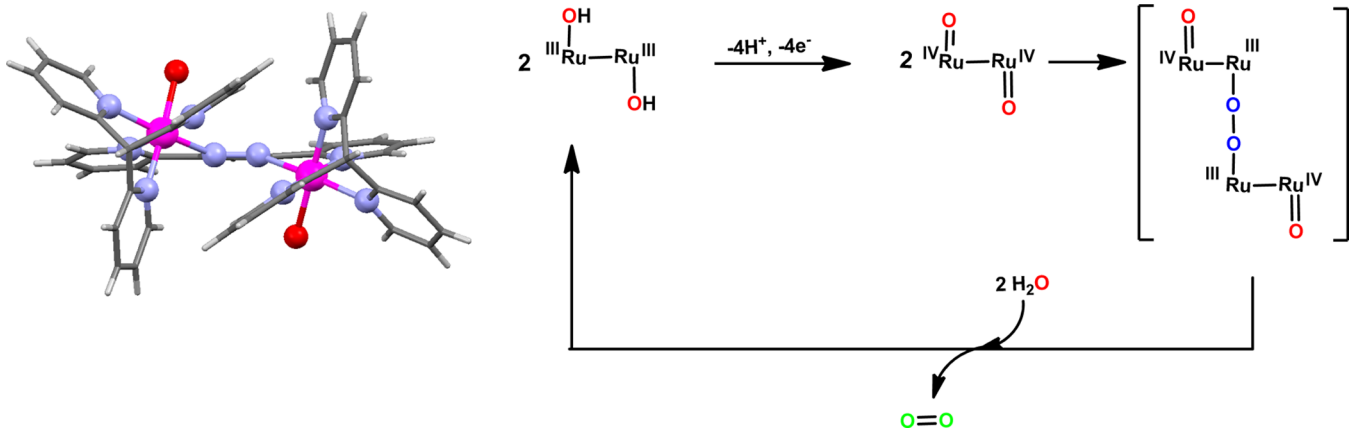

FIGURE 7. (left) Crystal structure of *trans*-{[Ru^{II}(tpym)(H_2O)]$_2$(μ-bpp)}$^{3+}$, **11**$^{3+}$. (right) Proposed intermolecular I2M mechanism.

evidence advocates for a WNA mechanism once each of the Ru centers of the complex reaches oxidation state V.

4. Interaction of Two M−O Units, I2M

4.1. Intramolecular I2M. The *in,in*-{[Ru^{II}(trpy)(H_2O)]$_2$(μ-bpp)}$^{3+}$ complex, **10**$^{3+}$, consists of a dinucleating 3,5-bis-(2-pyridyl)pyrazolate anionic ligand (bpp$^-$), which acts as a backbone for two Ru metal centers, placing them in close proximity and further providing a route for electronic coupling between them. This arrangement also places the two O atoms at 2.48 Å producing an additional through space supramolecular interaction.[15] The $Ru(II)_2$ species is sequentially oxidized by 1 e$^-$ processes up to the $Ru(IV)_2$ oxidation state. At this stage, the complex advances to a peroxido intermediate, entropically favored due to the ligand preorganization, which later on evolves dioxygen via an intramolecular I2M mechanism as depicted in Figure 6.[16] The rds is proposed to be the transformation of the bridging peroxido intermediate, [Ru^{III}−OO−Ru^{III}], into the corresponding terminal peroxido [HO−$Ru^{III}Ru^{III}$−OOH]. This process is favored by the presence of an additional H_2O molecule that acts both as a proton donor and as a proton acceptor, as shown in Figure 6. A new Ru dinuclear complex containing a bis-trpy-anthracene bridging ligand is also proposed to follow a similar mechanism.[17]

4.2. Intermolecular I2M. The dinuclear Ru complex *trans*-{[Ru^{II}(tpym)(H_2O)]$_2$(μ-bpp)}$^{3+}$, **11**$^{3+}$ (tpym = tris-2-pyridylmethane),[18] is electronically similar to **10**$^{3+}$, but the relative disposition of the Ru−aqua groups has been drastically changed (see Figure 7). Whereas for **10**$^{3+}$ the Ru−aqua are facing one another and interacting through space, in **11**$^{3+}$ the Ru−aqua groups are *trans* to one another and thus preclude an intramolecular interaction. Therefore based only on geometrical grounds, the O−O bond formation step for this new complex can only occur either by a WNA or by an intermolecular I2M interaction. Kinetics and ^{18}O labeling experiments clearly show that when the [O=Ru^{IV}−Ru^{IV}=O] species is reached a bimolecular process takes place generating a putative tetranuclear intermediate, bridged by a peroxido ligand as indicated in Figure 7. This preference for the I2M mechanism indicates the radical character of the Ru−O group in high oxidation states before the coupling occurs.

A new family of Ru complexes containing the dianionic tetranucleating [2,2′-bipyridine]-6,6′-dicarboxylato ligand (bdc^{2-}) of general formula *trans*-[Ru^{II}(bdc)(L)$_2$] (L = 4-Me-pyridine, **12a**; L = isoquinoline (isoq) **12b**) have been reported very recently.[19] The bdc^{2-} ligand occupies the equatorial position, whereas the monodentate pyridyl derivative ligands are situated at the axial positions, as can be seen in Figure 8. The dianionic nature of bdc^{2-} strongly lowers the redox potentials of the Ru center, and as a consequence higher oxidation states such as Ru(V) are easily accessible both thermodynamically and kinetically. The bdc^{2-} also produces an interesting geometrical effect, since the ORuO angle for **12a** is 124°, which is 34° away from the ideal octahedral geometry. This distortion of the equatorial angle allows it to achieve a seven coordinated [Ru^{IV}−OH] intermediate upon reaching oxidation state IV as can be seen in the crystal structure of *trans*-[Ru^{IV}(bdc)(Me-4-py)$_2$(OH)]$^+$ and in the calculated structure of *trans*-[Ru^{V}(bdc)(isoq)$_2$(O)]$^+$ depicted in Figure 8. At lower oxidation states, it is proposed based on DFT that in water an aqua ligand coordinates at the expense of one of the pyridyl bdc^{2-} N-atoms, maintaining a typical hexacoordinated octahedral type of geometry. One of the most interesting features of this complex is this capacity of the bdc^{2-} ligand to adapt to the electronic demands of the Ru metal in different oxidation states,

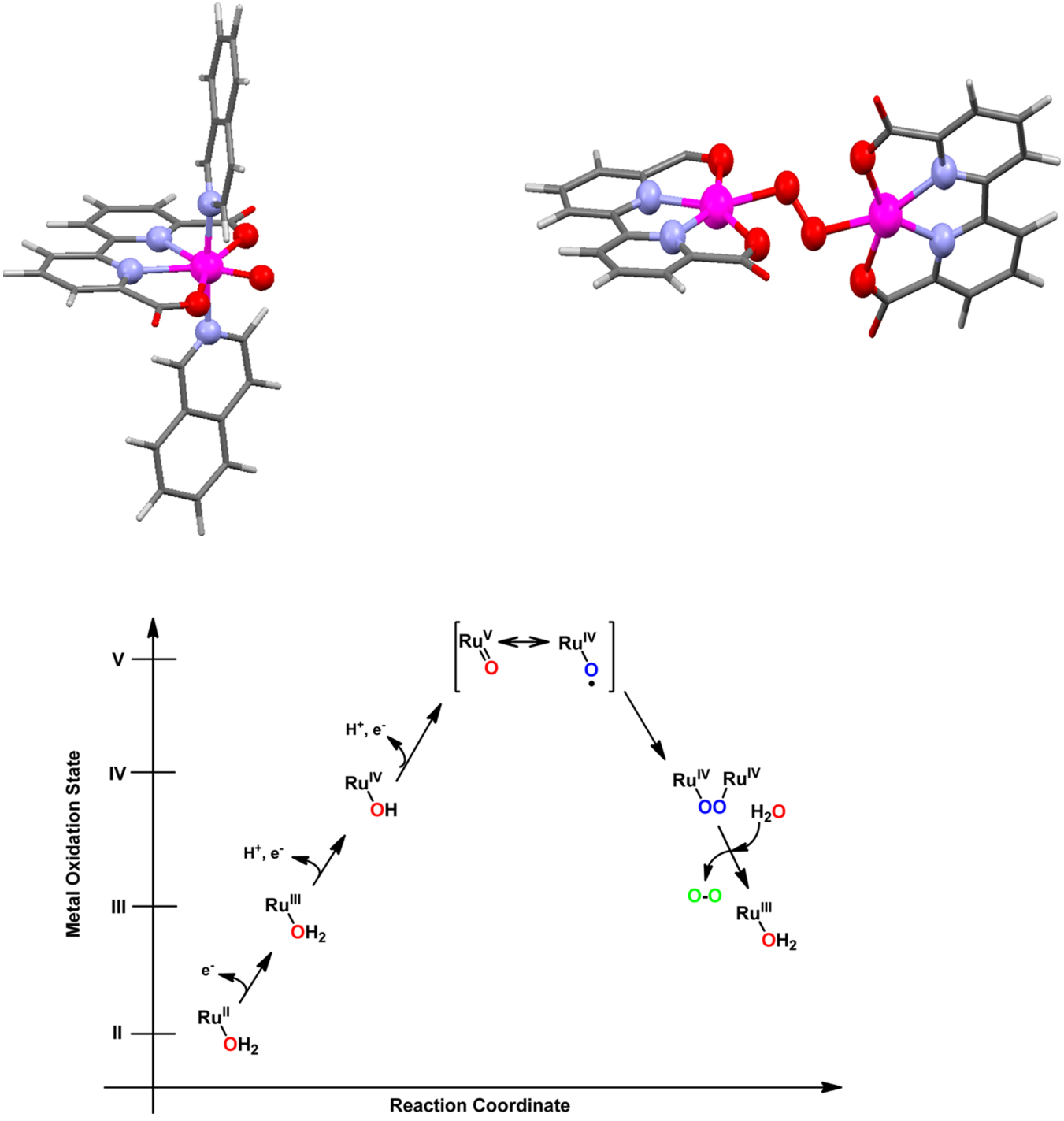

FIGURE 8. (top, left) Capped stick representation of $[Ru^{V}(bdc)(isoq)_2(O)]^{+}$ DFT calculated structure. (top, right) The transition state structure for the O–O bond formation step for $[Ru^{V}(bdc)(Me\text{-}4\text{-}py)_2(O)]^{+}$ (axial ligands are omitted). (bottom) Water oxidation intermolecular I2M mechanism catalyzed by **12**.

without reaching complete decoordination from the metal center. Additional one-electron oxidation to Ru(V) produces the dimerization of the complex forming the corresponding peroxido intermediate, $[^{IV}Ru{-}OO{-}Ru^{IV}]$ via an I2M mechanism. DFT calculations show that the former $[Ru^{V}{=}O]$ complex has a large degree of oxyl character $[Ru^{IV}{-}O^{\bullet}]$ and thus favors the dimerization process. This dimerization process is further favored in **12b** by the isoquinoline ligand through $\pi{-}\pi$ stacking interactions. The next step is the reductive elimination of the bridging peroxido ligand bonded to the two metals to form dioxygen with concomitant formation of the $[Ru^{III}{-}OH_2]$ species closing the catalytic cycle. This reductive process is not favored by the strong σ-donation nature of the bdc^{2-} ligands and is actually the rds. However

the fact that the reduction process takes place simultaneously at the two centers strongly reduces the energetic demands, and thus the whole catalytic cycle is still very fast. The seven coordination nature of the dimeric intermediate also weakens the Ru−O bond due to a diminished overlap of the O orbitals with the metal d orbitals under this geometry as compared with an ideal octahedral complex, thus favoring the kinetics of the substitution process. Under excess of a strong oxidant such as Ce(IV), the peroxido intermediate is further oxidized to the corresponding [Ru^{IV}−OO−Ru^{V}] peroxido or the superoxido [Ru^{IV}−OO−Ru^{IV}]. This complex is today the fastest WOC ever reported. Finally it is interesting to note that the removal of bpy by 1,10-phenanthroline in bdc^{2-} changes the mechanism to WNA due to the rigidity of the new aromatic framework, which does not allow the adaptative process to occur, thus habilitating the WNA pathway.[20]

5. Deactivation Pathways

Potential deactivation pathways for molecular WOCs are ligand oxidation, ligand decoordination, and a combination of both. Additionally these processes can end up forming oxides that can generate nanoparticulate aggregates or remain in solution depending on the pH and the transition metal used.

Ligand oxidation is an important side reaction in WO catalysis due to the high redox potential involved (eq 2). As a consequence of this, a catalyst that has the thermodynamic driving force to oxidize water to dioxygen will also be capable of oxidizing a whole range of organic substrates. In addition, the oxidation of organics by complexes containing the M−O or M−OO groups in high oxidation states can be very efficient as has been extensively described[21] for a variety of transition metals. Therefore in order to generate true molecular WOCs, it is absolutely indispensable to use oxidatively rugged ligands.

Deactivation pathways described for Ru WOCs in homogeneous phase are proposed to be due to bimolecular catalyst−catalyst interactions. In this way, the [Ru=O] or [RuOOH] active site of one catalyst molecule reacts with the ligand backbone of another molecule of the same catalyst. This deactivation pathway has been proposed to occur in tetranuclear Ru complexes[22] and in mononuclear complexes like [Ru^{II}(TPA-bpy)(H_2O)]$^{2+}$, $\mathbf{13}^{2+}$ (TPA-bpy = 1-([2,2′-bipyridin]-6-yl)-*N*,*N*-bis(pyridin-2-ylmethyl)methanamine), reported recently.[23] In both cases, the ligands used contain benzylic or pyridyl-benzylic CH_2 groups that are easily oxidized. Furthermore, in both cases, the formation of O_2 is accompanied by CO_2 and thus indicates that once the ligand oxidation starts a series of chain reactions lead to the total oxidation of the ligand. This process can be in some cases associated with the formation of RuO_2 nanoparticles that might end up being responsible for all the oxygen observed.

Ligand oxidation can also occur in an intramolecular manner as proposed with Ir complexes containing the facial Cp* (pentamethylcyclopentadienyl) ligand such as [Ir^{III}(Cp*)(bpy)Cl]$^{+}$, $\mathbf{14}^{+}$.[24] In this case, the potential [Ir^{V}−OOH] or the [Ir^{V}−O] groups have the perfect geometry to interact with the C−Me moiety of the Cp* ligand (See Figure 9). This has been further confirmed by the presence of HCOOH and MeCOOH during oxygen evolution and supported by DFT.

As mentioned above, besides ligand oxidation, another deactivation pathway that can occur is ligand decoordination. This is especially important for first raw transition metals where in general metal−ligand bonds are much more labile than those in Ru complexes, especially in water. For Fe complexes containing pyridyl-amine type of ligands, decoordination occurs at acidic pHs. For instance for the complex [Fe(N4Py)(CH_3CN)]$^{2+}$, $\mathbf{15}^{2+}$[25] (N4py = 1,1-di-(pyridin-2-yl)-*N*,*N*-bis(pyridin-2-ylmethyl)methanamine), and [Fe(BQEN)($OTf)_2$], **16**[26] (BQEN = *N*,*N*′-dimethyl-*N*,*N*′-bis(8-quinolyl)ethane-1,2-diamine), it has been reported that below pH 3.0 the only species present in solution are [$Fe^{II}(H_2O)_6$]$^{2+}$ and the free ligand. Thus when Ce(IV) is added, a pH decrease to approximately 1 takes place, and a series of decoordination equilibria similar to the ones shown in Figure 9 occur. In addition in this system, the formation of CO_2 takes place at the very beginning of the reaction together with the formation of O_2, indicating the presence of ligand oxidation pathways. Oxidative pathways for tertiary amines and pyridyl-benzyl CH_2 functionalities are well documented. The combination of all these degradative pathways, namely ligand oxidation and ligand decoordination upon addition of Ce(IV), generates dozens of potential species in different oxidation states that can coexist in solution. For this reason, a reliable molecular mechanism cannot be derived from these systems. On the other hand, it is important to keep in mind that ferrates in equilibrium with diferrates can potentially play a major role in oxygen evolution as has been reported recently.[27] At pH higher than 7, the system basically instantaneously forms Fe oxide/hydroxide nanoparticles (NP) that are responsible for the water oxidation activity.[28]

The formation of NP oxides from molecular complexes based on Mn, Fe, Co, Cu, and Ir[29] is, no wonder, one of the major discussions nowadays in this field. Reaction

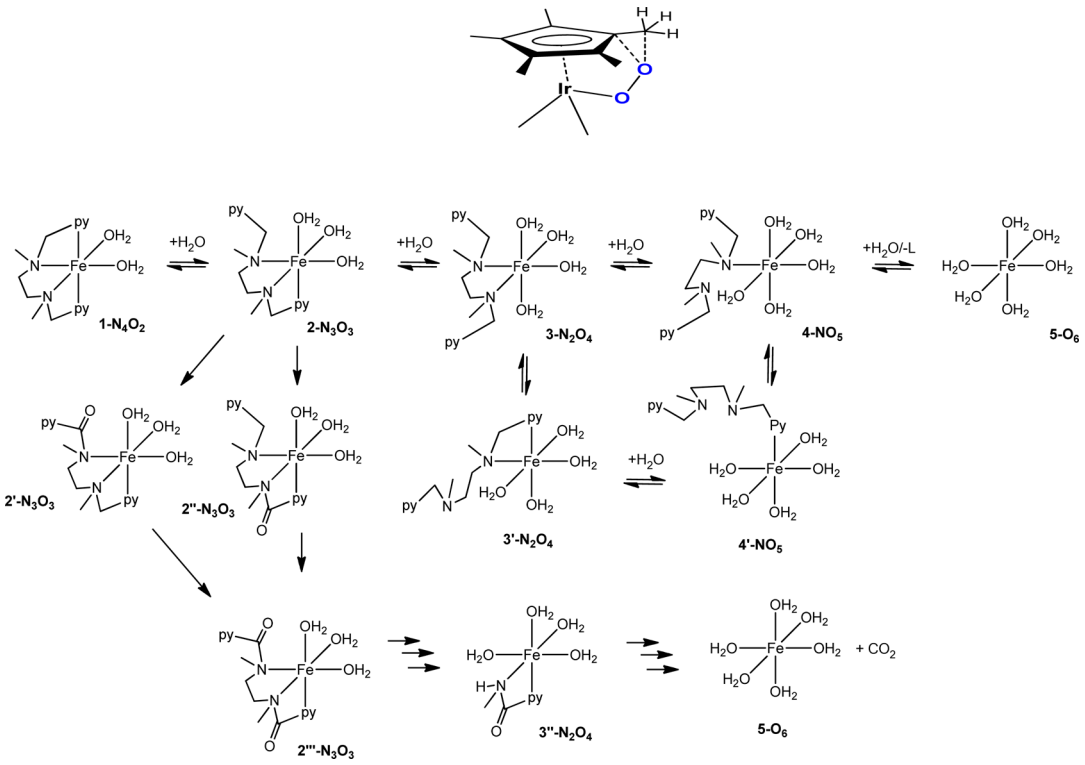

FIGURE 9. (top) Initial step for the degradation pathways of Ir complexes containing the facial Cp* ligand. (bottom) General degradation pathways proposed for Fe complexes containing pyridyl/amine ligands.

conditions, ligand ruggedness, and sacrificial oxidants are the main players that can influence the formation of oxides.

6. Conclusions

From the mechanistic description, it is clear that ligand design plays one of the major roles in the performance of the catalysts in terms of kinetics, turnover numbers, and deactivation pathways. There is an interplay between the electronic perturbation exerted by the ligand and the availability and stability of high oxidation states. In addition, given the redox nature of the catalytic cycle, there is always a combination of pathways involving both oxidations and reductions. Therefore any perturbation that favors the oxidative side will disfavor the reductive one. Thus the key issue here will be to know which step or steps are the rds so that appropriate ligands can be designed accordingly. Another key point in water oxidation catalysis is the need to activate the transition metal to reach higher oxidation states. For the particular case of Ru in general, any oxidation state higher than III will involve the oxidation of both the Ru center and the oxygen atom of the Ru−O group. This will have dramatic consequences with regard to the reactivity of the generated species and also with regard to the potential O−O bond formation pathway. Intuitively, the more radical the character of oxygen the higher the chances for the I2M mechanism and the other way around. And finally another issue in which ligands are also crucial is the kinetics of substitution needed for aqua ligand coordination and oxygen ejection, especially when they are involved in the rds.

Besides the direct electronic effects mentioned above, the ligands can also be responsible for supramolecular through space type of interactions as well as for second coordination sphere effects, which can strongly influence the overall performance of the catalyst. The ligands can also have a strong impact in the coordination geometry of the metal center, which is nicely exemplified by the case of a seven coordinated Ru in high oxidation states.

Another important effect is the presence of multiple $Ru-OH_2$ groups available per metal center as well as the presence of bridging ligand that allow a certain degree of electronic coupling among them. There are a large variety of bridging ligands that can exert space and electronic effects, and accordingly a huge variety of potential catalysts can be envisaged.

There are some other interrelated challenges the field is facing today. One of them is the proper spectroscopic and electronic characterization of reaction intermediates in water. This is intrinsically difficult since the important

intermediates are also the most reactive ones and thus the more difficult to characterize. Therefore theory should play here a very important role. Also during the last 5 years, molecular WOCs have experienced a huge improvement with regard to kinetics, and we have managed to obtain catalysts that evolve O_2 as fast as the OEC-PSII, although they deactivate very quickly. Thus another important challenge is to be able to make fast and long-lasting catalysts, so that they can approach potential commercializable devices. Here the knowledge of the mechanistic paths that derail the productive ones is fundamental in order to come up with better catalysts. Finally all the WOCs that have been reported until now are proposed to take place through pathways involving peroxide intermediates. In sharp contrast in Nature the proposed mechanistic pathway for the OEC-PSII involves a concerted $4e^-$ process directly to O_2 with the obvious thermodynamic benefit. Here again the knowledge of how the ligands influence the electronic structure of the metal centers can indicate potential ways of achieving such a concerted pathway.

In conclusion, the combination of transition metals and auxiliary and bridging ligands constitute a fabulous toolkit that properly used should allow us to generate the needed rugged and efficient WOCs, which could be incorporated into a successful photoelectrochemical cell for overall water splitting using sunlight. A very important part of this knowledge will certainly come from the mechanistic description. In addition, this knowledge is also very useful in order to shed light on possible reaction pathways that take place in more complex systems such as the OEC-PSII or in the solid state systems where intermediates are much more difficult to characterize.[30]

Support from Generalitat de Catalunya (Grant 2009 SGR-69), MINECO (Grants CTQ-2010-21497, CTQ2011-26440, and PRI-PIBIN-2011-1278), and "La Caixa" Foundation is gratefully acknowledged. Jonathan De Tovar is thanked for creating the conspectus artwork.

BIOGRAPHICAL INFORMATION

Xavier Sala was born in Sant Feliu de Guíxols in 1979 and received a Ph.D. in Chemistry from UdG in 2007. After postdoctoral research with P. W. N. M. van Leeuwen and A. Llobet at ICIQ, he is currently Lecturer at UAB, where he leads the SelOxCat research group.

Somnath Maji received his Ph.D. in 2009 from I.I.T. Bombay, India, under the supervision of G. K. Lahiri. Henceforth he is a postdoctoral researcher in Antoni Llobet's group at ICIQ, Tarragona, Spain. Currently he is working on all aspects of ruthenium complexes that catalyze water oxidation.

Roger Bofill, born in Catalonia (Spain) in 1973, obtained the degree and Ph.D. in Chemistry at the UAB. He was a postdoctoral researcher at the universities of Sussex and Nottingham (UK) during 2001−2004, and he is currently Lecturer at the UAB, working on selective oxidation catalysis.

Jordi García-Antón was born in Cubelles (Barcelona, Spain) in 1976. He received his Ph.D. in Chemistry in 2003 from the UAB. After a postdoctoral stay at the LCC−CNRS in Toulouse (France) in the group of Bruno Chaudret, he joined the UAB as a Lecturer in chemistry.

Lluis Escriche was born in Manresa, Spain, in 1957. He received B.S. and Ph.D. degrees in chemistry from the UAB, and since 1990, he has been associate professor of Inorganic Chemistry at this university.

Antoni Llobet received a Ph.D. from UAB. Then he was a Post-Fellow at the University of North Carolina with T.J. Meyer and at Texas A&M University with D.T. Sawyer and A.E. Martell. He is currently a Professor of Chemistry at UAB and Group Leader at ICIQ.

FOOTNOTES

The authors declare no competing financial interest.
Dedicated to the memory of Prof. Joan Sola i Casadevall, excellent lecturer of Chemistry at the Universitat Autònoma de Barcelona (UAB).

REFERENCES

1 Barber, J. Photosynthetic energy conversion: Natural and artificial. *Chem. Soc. Rev.* **2009**, *38*, 185–196.

2 Meyer, T. J.; Huynh, M. H. V. The remarkable reactivity of high oxidation state ruthenium and osmium polypyridyl complexes. *Inorg. Chem.* **2003**, *42*, 8140–8160.

3 Lee, A. Q.; Streit, B. R.; Zdilla, M. J.; Abu-Omar, M. M.; DuBois, J. L. Mechanism of and exquisite selectivity for O-O bond formation by the heme-dependent chlorite dismutase. *Proc. Natl. Acad. Sci. U. S. A.* **2008**, *105*, 15654–15659.

4 Cao, R.; Lai, W.; Du, P. Catalytic water oxidation at single metal sites. *Energy Environ. Sci.* **2012**, *5*, 8134–8157.

5 Vigara, L.; Ertem, M. Z.; Planas, N.; Bozoglian, F.; Leidel, N.; Dau, H.; Haumann, M.; Gagliardi, L.; Cramer, C. J.; Llobet, A. Experimental and quantum chemical characterization of the water oxidation cycle catalysed by $[Ru^{II}(damp)(bpy)(H_2O)]^{2+}$. *Chem. Sci.* **2012**, *3*, 2576–2586.

6 Murakami, M.; Hong, D.; Suenobu, T.; Yamaguchi, S.; Ogura, T.; Fukuzumi, S. Catalytic mechanism of water oxidation with single-site ruthenium−heteropolytungstate complexes. *J. Am. Chem. Soc.* **2011**, *133*, 11605–11613.

7 Chen, Z.; Concepcion, J. J.; Hu, X.; Yang, W.; Hoertz, P. G.; Meyer, T. J. Concerted O atom−proton transfer in the O-O bond forming step in water oxidation. *Proc. Natl. Acad. Sci. U. S. A.* **2010**, *107*, 7225–7229.

8 Wasylenko, D. J.; Ganesamoorthy, C.; Henderson, M. A.; Koivisto, B. D.; Osthoff, H. D.; Berlinguette, C. P. Electronic modification of the $[Ru^{II}(tpy)(bpy)(OH_2)]^{2+}$ scaffold: Effects on catalytic water oxidation. *J. Am. Chem. Soc.* **2010**, *132*, 16094–16106.

9 Maji, S.; Lopez, I.; Bozoglian, F.; Benet-Buchholz, J.; Llobet, A. Mononuclear ruthenium−water oxidation catalysts: Discerning between electronic and hydrogen-bonding effects. *Inorg. Chem.* **2013**, *52*, 3591–3593.

10 Yamazaki, H.; Hakamata, T.; Komi, M.; Yagi, M. Stoichiometric photoisomerization of mononuclear ruthenium(II) monoaquo complexes controlling redox properties and water oxidation catalysis. *J. Am. Chem. Soc.* **2011**, *133*, 8846–8849.

11 Boyer, J. L.; Polyansky, D. E.; Szalda, D. J.; Zong, R.; Thummel, R. P.; Fujita, E. Effects of a proximal base on water oxidation and proton reduction catalyzed by geometric isomers of $[Ru(tpy)(pynap)(OH_2)]^{2+}$. *Angew. Chem., Int., Ed.* **2011**, *50*, 12600–12604.

12 Sala, X.; Ertem, M. Z.; Vigara, L.; Todorova, T. K.; Chen, W.; Rocha, R. C.; Cramer, C. J.; Gagliardi, L.; Llobet, A. The cis-$[Ru^{II}(bpy)_2(H_2O)_2]^{2+}$ water-oxidation catalyst revisited. *Angew. Chem., Int. Ed.* **2010**, *49*, 7745–7747.

13 Gilbert, J. A.; Eggleston, D. S.; Murphy, W. R., Jr.; Geselowitz, D. A.; Gersten, S. W.; Hodgson, D. J.; Meyer, T. J. Structure and redox properties of the water-oxidation catalyst $[(bpy)_2(OH_2)RuORu(OH_2)(bpy)_2]^{4+}$. *J. Am. Chem. Soc.* **1985**, *107*, 3855–3864.

14 Sartorel, A.; Miró, P.; Salvadori, E.; Romain, S.; Carraro, M.; Scorrano, G.; Di Valentin, M.; Llobet, A.; Bo, C.; Bonchio, M. Water oxidation at a tetraruthenate core stabilized by

polyoxometalate ligands: Experimental and computational evidence to trace the competent intermediates. *J. Am. Chem. Soc.* **2009**, *131*, 16051–16053.

15 Romain, S.; Bozoglian, F.; Sala, X.; Llobet, A. Oxygen-oxygen bond formation by the Ru-Hbpp water oxidation catalyst occurs solely via an intramolecular reaction pathway. *J. Am. Chem. Soc.* **2009**, *131*, 2768–2769.

16 Bozoglian, F.; Romain, S.; Ertem, M. Z.; Todorova, T. K.; Sens, C.; Mola, J.; Rodríguez, M.; Romero, I.; Benet-Buchholz, J.; Fontrodona, X.; Cramer, C. J.; Gagliardi, L.; Llobet, A. The Ru-Hbpp water oxidation catalyst. *J. Am. Chem. Soc.* **2009**, *131*, 15176–15187.

17 Wada, T.; Ohtsu, H.; Tanaka, K. Catalytic four-electron oxidation of water by intramolecular coupling of the oxo ligands of a bis(ruthenium−bipyridine) complex. *Chem.—Eur. J.* **2012**, *18*, 2374–2381.

18 Maji, S.; Vigara, L.; Cottone, F.; Bozoglian, F.; Benet-Buchholz, J.; Llobet, A. Ligand geometry directs O-O bond formation pathway in new trans-RuHbpp based water oxidation catalyst. *Angew. Chem., Int. Ed.* **2012**, *51*, 5967–5970.

19 Duan, L.; Bozoglian, F.; Mandal, S.; Stewart, B.; Privalov, T.; Llobet, A.; Sun, L. A molecular ruthenium catalyst with the water-oxidation activity comparable to that of photosystem II. *Nat. Chem.* **2012**, *4*, 418–423.

20 Lianpeng, T.; Duan, L.; Xu, Y.; Privalov, T.; Sun, L. Structural modifications of mononuclear ruthenium complexes: A combined experimental and theoretical study on the kinetics of ruthenium-catalyzed water oxidation. *Angew. Chem., Int. Ed.* **2011**, *50*, 445–449.

21 Nam, W. High-valent iron(IV)-oxo complexes of heme and non-heme ligands in oxygenation reactions. *Acc. Chem. Res.* **2007**, *40*, 522–531.

22 Francas, L.; Sala, X.; Escudero-Adan, E.; Benet-Buchholz, J.; Escriche, L.; Llobet, A. Synthesis, structure, and reactivity of new tetranuclear Ru-Hbpp-based water-oxidation catalysts. *Inorg. Chem.* **2011**, *50*, 2771–2781.

23 Radaram, B.; Ivie, J. A.; Singh, W. M.; Grudzien, R. M.; Reibenspies, J. H.; Webster, C. E.; Zhao, X. Water oxidation by mononuclear ruthenium complexes with TPA-based ligands. *Inorg. Chem.* **2011**, *50*, 10564–10571.

24 Savini, A.; Belanzoni, P.; Bellachioma, G.; Zuccaccia, C.; Zuccaccia, D.; Macchioni, A. Activity and degradation pathways of pentamethyl-cyclopentadienyl-iridium catalysts for water oxidation. *Green Chem.* **2011**, *13*, 3360–3374.

25 Draksharapu, A.; Li, Q.; Logtenberg, H.; van den Berg, T. A.; Meetsma, A.; Killeen, J. S.; Feringa, B. L.; Hage, R.; Roelfes, G.; Browne, W. E. Ligand exchange and spin state equilibria of Fe^{II}(N4Py) and related complexes in aqueous media. *Inorg. Chem.* **2012**, *51*, 900–913.

26 Hong, D.; Mandal, S.; Yamada, Y.; Lee, Y.-L.; Nam, W.; Llobet, A.; Fukuzumi, S. Water oxidation catalysis with nonheme-iron complexes under acidic and basic conditions: homogeneous or heterogeneous? *Inorg. Chem.* **2013**, *52*, 9522–9531.

27 Sarma, R.; M. Angeles-Boza, A. M-; Brinkley, D. W.; Roth, J. P. Studies of the Di-iron(VI) intermediate in ferrate-dependent oxygen evolution from water. *J. Am. Chem. Soc.* **2012**, *134*, 15371–15386.

28 Chen, G.; Chen, L.; Ng, S.-M.; Man, W.-L.; Lau, T.-C. Chemical and visible-light-driven water oxidation by iron complexes at pH 7−9: Evidence for dual-active intermediates in iron-catalyzed water oxidation. *Angew. Chem., Int. Ed.* **2013**, *52*, 1789–1791.

29 Hong, D.; Murakami, M.; Yamada, Y.; Fukuzumi, S. Efficient water oxidation by cerium ammonium nitrate with $[Ir^{III}(Cp^*)(4,4'\text{-bishydroxy-}2,2'\text{-bipyridine})(H_2O)]^{2+}$ as a precatalyst. *Energy Environ. Sci.* **2012**, *5*, 5708–5716.

30 Suntivich, J.; Gasteiger, H. A.; Yabuuchi, N.; Nakanishi, H.; Goodenough, J. B.; Shao-Horn, Y. Design principles for oxygen-reduction activity on perovskite oxide catalysts for fuel cells and metal-air batteries. *Nat. Chem.* **2011**, *3*, 546–550.